Int. J. Electrochem. Sci., 17 **(2022)** Article Number: 220342, doi: 10.20964/2022.03.43

International Journal of
ELECTROCHEMICAL
SCIENCE
www.electrochemsci.org

Mini review

Progress in Nanomaterials-based Electrochemical Biosensors for Beta-amyloid Peptides as the Biomarkers of Alzheimer's Disease

Yun-Xiao Feng[*] *and Chang-Dong Chen*[*]

College of Chemistry and Chemical Engineering, Pingdingshan University, Pingdingshan, Henan 467000, People's Republic of China
[*]E-mail: 2743@pdsu.edu.cn (Y.F.); qgfenghxx@163.com (C.C.)

Received: 23 December 2021 / *Accepted:* 17 January 2022 / *Published:* 2 February 2022

Alzheimer's disease (AD) have affected the older population worldwide through the rapid decline in cognitive impairment. Mounting evidence suggest that beta-amyloid peptide (Aβ) and its derivates are closely related to the emergence and growth of AD. Thus, the specific and sensitive detection of Aβ species have an important role in the early diagnosis of AD. Electrochemical method is a promising candidate for bioassays. The current review mainly focuses on the development of nanomaterials-based electrochemical biosensors for Aβ species in the past decades. We cover the comprehensive utilization of nanomaterials in biosensor construction as the electrode substrate and signal reporters.

Keywords: Alzheimer's disease; beta-amyloid peptide; electrochemical biosensor; nanomaterials

1. INTRODUCTION

Alzheimer's disease (AD) is a chronic and progressive central nervous system degenerative disease becoming more prevalent across the world. It has been reported that the generation of AD is closely related with the extracellular accumulation of amyloid β peptide (Aβ) in the brain [1, 2]. Aβ peptide is produced from the proteases-catalyzed hydrolysis of a larger amyloid precursor protein (APP) and consists of 39-42 amino acids. In contrast to abundant $A\beta_{1-40}$ peptide, $A\beta_{1-42}$ peptide is proved to be more crucial to the amyloid cascade hypothesis of AD. Moreover, during the nucleation-dependent process, Aβ peptide exhibits different forms, including monomer, oligomer (AβO) and fibril (AβF). Among different assembled states, AβO was considered to be associated with the severity of AD [3, 4]. Therefore, there is an intense necessary to develop effective methods for the accurate detection of Aβ species for the early diagnosis of AD [5].

Currently, enzyme-linked immunosorbent assay (ELISA) and western-blot immunoassay are applied in the clinical application [6, 7]. However, the test always confronts of several intrinsic

drawbacks, such as time consuming, intensive labour and low sensitivity. To meet the need of sensitive detection of ultra-low levels of Aβ in body fluids, various platforms based on different sensing techniques have been established, including fluorescence [8, 9], colorimetry [10, 11], surface plasmon resonance and surface enhanced Raman scattering [12], electrochemiluminescence [13, 14], photoelectrochemistry [15, 16] and mass spectrometry [17-19]. Among them, electrochemical methods have attracted numerous attention because of their striking merits of high selectivity, rapid response, low cost and easy operation [20-23]. Label-free methods are relative attractive in the field of Aβ analysis [24, 25]. Vestergaard et al. proposed a rapid label-free electrochemical method for the detection of Aβ aggregation based on the oxidation of the single Tyr residue in Aβ peptide as the signal reporter [26]. Besides, the binding of Aβ species to their aptamers can influence the surface electron transfer of the redox mediator to the electrode. Based on this principle, several label-free methods have been developed [27-38]. For example, Li et al. found that $A\beta_{1-42}$ oligomer binding with ferrocene (Fc)-labeled oligopeptide would slow down the surface electron transfer rate and resulted in the suppressed response at a higher frequency [39]. Zhang et al. reported that the binding of AβO changed the conformation of Fc-labeled stem-loop probes into "open" state and increased the distance between Fc and the electrode surface, leading to the decreased charge transfer current [40]. However, the low sensitivity heavily limited the application of this method. To further improve the sensitivity, signal amplification strategies were integrated into the assays of Aβ [41]. For instance, Liu's group introduced p-aminophenol redox cycling and alkaline phosphatase (ALP)-assisted electrochemical–chemical–chemical redox cycling into electrochemical bioassay of $A\beta_{1-42}$ and total Aβ peptide [42, 43]. Meanwhile, for multiplex detection, multichannel sensor array have been constructed [44, 45].

Nanotechnology advancements have provided an exceptional opportunity in the electrochemical assays of Aβ species with higher sensitivity and selectivity. Their inherent physiochemical properties make the signal transduction more efficient. In this review, nanomaterials-based electrochemical platforms for the determination of Aβ species are summarized according to the role of nanomaterials in the assay.

2. NANOMATERIALS-BASED ELECTROCHEMICAL BIOSENSORS

2.1 Nanomaterials as electrode matrices

Nanomaterials have been widely utilized as the functionalized materials to fabricate or modify the electrode for the enhancement of the sensitivity of electrochemical biosensors. Large surface area-volume ratio of nanomaterials favors the immobilization of high amount of biorecognition elements and improves the accessibility of targets to the receptors. Meanwhile, excellent electron conductivity and catalytic activity can accelerate the electron transfer and redox reaction on the surface of the electrode. Metal and metal oxide nanomaterials with various nanostructures are popularly used to modify the electrode and improve the detection efficiency because of their multifunctional properties, including excellent stability, high biocompatibility and large surface area [46-50]. The nanomaterials-based electrodes have been used for the detection of different Aβ species (Table 1). For example, saccharide-immobilized gold nanoparticles (AuNPs) were immobilized on the carbon electrode for the capture and detection of Aβ [51]. Rama et al. reported a competitive electrochemical immunosensor for the detection

of $A\beta_{1–42}$ peptide based on gold nanostructurated screen-printed carbon electrodes (SPCEs) [52]. Electrospun SnO_2 nanofibers were employed as the transducing material to modify the electrode for the electrochemical detection of $A\beta_{1–42}$ peptide [53]. Meanwhile, enzyme-based signal amplification strategies were introduced into the assay of Aβ peptide. Diba et al. proposed an sandwich-type electrochemical immunosensor for detection of Aβ peptide on the AuNPs-decorated SPCE [54]. Based on the different binding sites, anti-Aβ(12F4) was tethered on the electrode surface for the capture of Aβ peptide and ALP-labeled anti-Aβ (1E11) was employed as detection antibody. After the formation of immunocomplex, surface bounded ALP enzyme could catalyze the hydrolysis of substrate 4-amino phenyl phosphate (APP) into 4-aminophenol, producing a voltammetric detection signal. To increase the resisting nonspecific adsorption capability, Liu et al. modified superhydrophobic carbon fiber paper (CFP) with AuPt alloy NPs for the development of electrochemical aptasensor of AβO [55].

Carbon-based nanomaterials, such as graphene and carbon nanotubes, have been intensively utilized in the field of electrochemistry owing to their unique chemical and physical properties including high conductivity and ease of surface modification. Abbasi et al. developed a graphene-based electrochemical immunosensor for the label-free detection of $A\beta_{1–42}$ peptide [56]. For maintaining the excellent property of graphene and improving the sensing efficiency, 1,5-diaminonaphthalene (pDAN) polymer was attached on the electrode surface for the binding of antibody. Sethi et al. designed a label-free biosensor for $A\beta_{1–42}$ peptide based on graphene and reduced graphene oxide dual-layer [57]. To further enhance the sensing performance, plenty of nanocomposites of graphene and other nanomaterials are designed and synthesized as the electrode materials for Aβ detection. AuNPs and nickel ferrite-decorated GO-chitosan nanocomposites were prepared for the development of immunosensor of $A\beta_{1–42}$ peptide [58]. Magnetic nitrogen-doped graphene (MNG) was used to modify the gold electrode for non-invasive detection of $A\beta_{1–42}$ peptide [59].

Table 1. Analytical performances of different electrodes for Aβ detection.

Electrode Modifier	Target	Detection limit	Linear range	Ref.
microporous gold nanostructure	$A\beta_{1–42}$	0.2 pg/mL	0.003–7 ng/mL	[46]
fern leaves-like gold nanostructure	$A\beta_{1–42}$	0.4 pg/mL	0.002–1.28 ng/mL	[47]
AuNPs	AβF	0.6 pM	0.5–4.0 pM	[48]
hierarchical gold dendrite	AβO	1 aM	10^{-9}–10 nM	[49]
HRP-AuNPs-gelsolin	$A\beta_{(1-40/1-42)}$	28 pM	0.1–50 nM	[50]
AuNPs	$A\beta_{1–42}$ and $A\beta_{1–40}$	1 μM	Not reported	[51]
AuNPs	$A\beta_{1–42}$	100 pg/mL	0.5–500 ng/mL	[52]
electrospun SnO_2 nanofibers	$A\beta_{1–42}$	1.46×10^{-7} pg/mL	1×10^{-6}–1000 ng/mL	[53]
AuNPs	$A\beta_{1–42}$	Not reported	0.1–25 pM	[54]
AuPt alloy nanoparticles	AβO	0.16 pg/mL	0.0005–10 ng/mL	[55]
graphene	$A\beta_{1–42}$	1.4 pg/mL	0.001–1 ng/mL	[56]
graphene and rGO dual-layer	$A\beta_{1–42}$	2.398 pg/mL	0.011–55 nM	[57]
AuNPs/$NiFe_2O_4$@GO-Ch	$A\beta_{1–42}$	3 pg/mL	0.001–1 ng/mL	[58]
MNG	$A\beta_{1–42}$	5 pg/mL	0.005-0.8 ng/mL	[59]

Abbreviation: AuNPs, gold nanoparticles; HRP, horseradish peroxidase; AβO, Aβ oligomer; rGO, reduced graphene oxide; GO, graphene oxide; Ch, chitosan; MNG, magnetic nitrogen-doped graphene.

2.2 Nanomaterials as signal reporters

Gold nanomaterials with excellent conductivity and catalytic properties can accelerate the electron communication between redox mediator and electrode. They have been used as the signal reporters or carriers for the detection of different Aβ species. For example, Liu's group found that a PrP peptide can be used as the receptor of AβO and the trigger of AuNPs assembly on the electrode surface [60]. The formed AuNPs-based network could significantly decrease the charge transfer resistance. Once the peptide on the electrode surface was bound with AβO, the formation of peptide-AuNPs network was inhibited and the charge transfer resistance obviously increased. Recently, Wang et al. reported an electrochemical aptasensor for AβO based on the target-modulated triple-helix aptamer switch (THAS) [61]. In this work, signal transduction DNA probes on AuNPs surface could hybridize with two symmetrical arm sequences conjugated on the two ends of aptamers into THAS. With the aid of trithiocyanuric acid (TA), network-like TA/AuNPs was in-situ formed on the electrode surface, leading to the enhancement of DPV responses. The interaction between AβO and aptamer broke the structure of THAS and AuNPs and made them dissociated from the electrode, thus causing a decline of DPV signal.

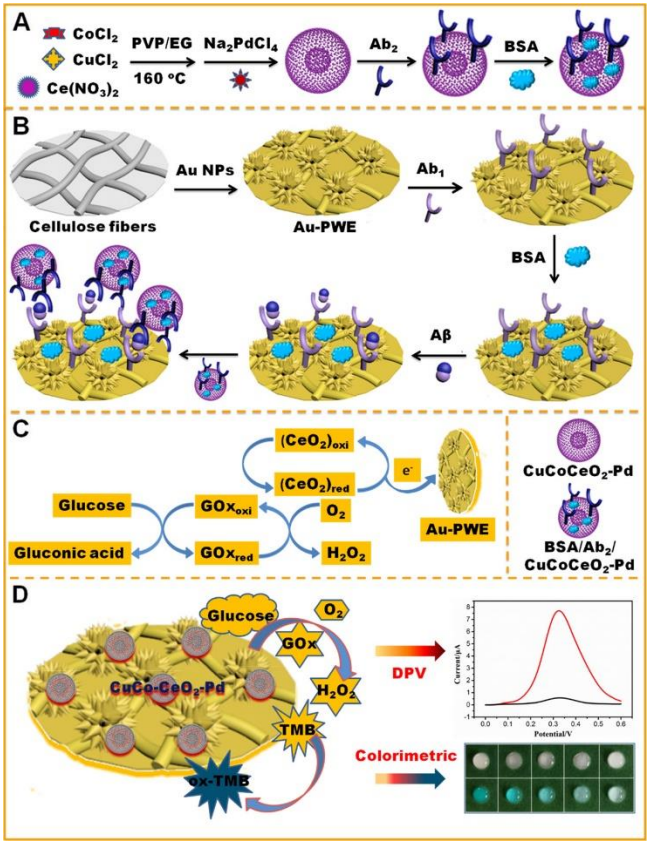

Figure 1. Schematic illustration of the synthesis of CuCo-CeO_2-Pd nanospheres and the immobilization of Ab_2 (**A**); The construction procedures of oPAD (**B**); The dual-mode sensing principle with DPV signal amplification and colorimetric reaction for Aβ determination (C, D) [62]. Copyright 2021 American Chemical Society.

Nanomaterials with good electrocatalytic ability can be introduced into electrochemical biosensors as the signal reporters for signal amplification. For instance, Escosura-Muñiz developed an electrochemical immunosensor for Aβ detection based on the electrocatalytic capability of AuNPs towards hydrogen evolution reaction (HER) [63]. Liu's group reported an electrochemical immunosensor for the detection of total Aβ peptides by using $Aβ_{1-16}$-heme-modified AuNPs [64]. In this work, $Aβ_{1-16}$-heme complex on the surface displayed the electrocatalytic ability toward O_2 reduction reaction. After the pre-incubation of the monoclonal antibody (mAb)-covered gold electrode with Aβ peptides, $Aβ_{1-16}$-heme-modified AuNPs were captured by the free mAb to catalyze the reduction of dissolved O_2 into H_2O_2. The generated reduction current signal was in inverse proportion to the concentration of total Aβ peptides in samples. Owing to the coexisting dual oxidation state (Ce^{3+} and Ce^{4+}), CeO_2 not only possesses the excellent catalytic properties but also acts as a redox mediator to generate detectable electrochemical signals. Recently, Cui et al. constructed an origami paper-based analytical device (oPAD) by using Pd decoraed Cu/Co-doped CeO_2 (CuCo-CeO_2-Pd) nanospheres for dual-mode electrochemical and visual detection of Aβ [62]. As shown in Figure 1, for extra oxygen vacancies and uniform nanosize morphology, CeO_2 was doped with Cu and Co elements and then in-situ decorated with Pd. The urchin-like AuNP layer was in-situ produced onto the cellulose fibers for the modification of anti-Aβ. After the immunoreaction, CuCo-CeO_2-Pd with outstanding electrocatalytic ability could generate electrochemical and colorimetric signal. To avoid the use of relatively unstable enzyme, Cu_xO was used to functionalize mesoporous CeO_2 to catalyze the decomposition of H_2O_2 and amplify the signal for immunosensing Aβ [65].

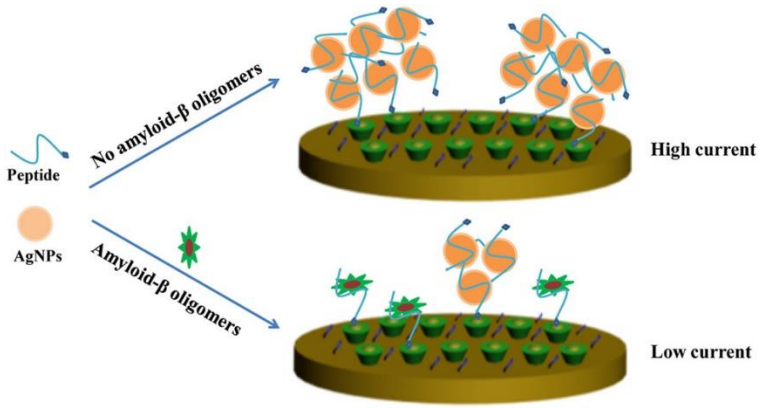

Figure 2. Schematic illustration of the electrochemical method for the selective detection of AβO using AgNPs as the redox reporters and Ad-PrP(95−110) as the receptor [66]. Copyright 2016 American Chemical Society.

In recent years, nanomaterials that can be directly used as signal probes have aroused the wide interest in bioassays [67]. For example, Zhou et al. reported the electrochemical assay of AβO based poly(thymine)-templated Cu nanoparticles as signal probes [68]. Metal organic frameworks (MOFs) were assembled with metal ions as the nodes and organic legends as the linkers. Through careful choice of elements, electroactive Cu-based and Zn-based MOFs with nanostructures were prepared and applied for electrochemical analysis [69]. Furthermore, Wang et al. presented an electrochemical aptasensor for AβO detection based on Cu-MOF and triple helix switch [70]. In this study, AuNPs@CuMOF

synthesized through a "one-pot" method was labeled with signal displaced-probe (SD). AuNPs@CuMOF/SD could hybridize with anti-AβO aptamer on the electrode surface to form triple helix switch (THS). In the presence of AβO, the structure of THS was destroyed and AuNPs@CuMOF/SD was liberated from the surface of the electrode, leading to the decrease of the strong signal of differential pulse voltammetry (DPV). Xia et al. reported an electrochemical biosensor for the detection of AβO by the in-situ assembled network of silver nanoparticles (AgNPs) as the redox reporter for signal amplification [66]. As displayed in Figure 2, adamantine-labeled PrP(95−110) denoted as Ad-PrP(95−110) could induce the aggregation of AgNPs into network architectures. Then, the formed Ad-PrP(95−110)-AgNPs networks were tethered on the β-cyclodextrin (β-CD)-modified gold electrode through the host-guest interaction between Ad and β-CD, thus producing a well-defined and sharp electrochemical signal through the solid-state Ag/AgCl reaction by AgNPs. However, in the presence of AβO, Ad-PrP(95−110) specifically bound to AβO with high affinity and lose the ability to trigger the assembly of AgNPs on the electrode surface, subsequently resulting in the decrease of the electrochemical signal.

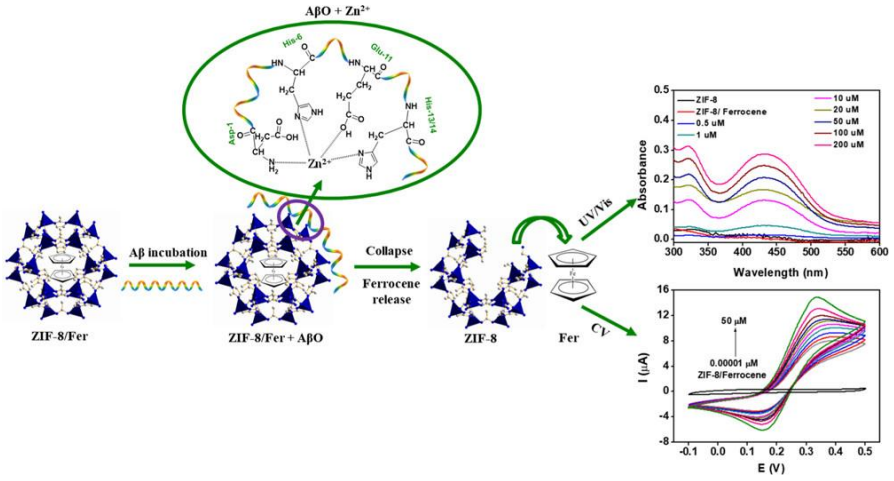

Figure 3. Schematic illustration of the nanoscale ZIF-8/Fc for AβOs sensing using optical and electrochemical methods [71]. Copyright 2019 American Chemical Society.

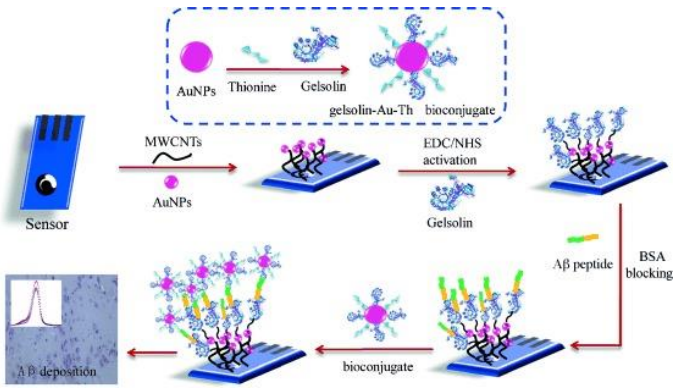

Figure 4. Schematic illustration of the electrochemical detection of $A\beta_{(1\text{-}40/1\text{-}42)}$ by using a gelsolin-Au-Th bioconjugate as a probe [72]. Copyright 2019 American Chemical Society.

Electroactive molecules such as Fc, thionine (Th) and metal ions can be loaded into or on the surface of nanomaterials to produce remarkable signal [73, 74]. Han et al. reported a sensitive electrochemical immunoassay of Aβ by using Fc-modified MOF as the signal tag [75]. In this work, high-content Fc molecules were covalently bonded in the Zn-MOF through the postsynthetic modification to prevent the leakage of signal molecules. Qin et al. employed Fc-loaded zeolitic imidazole framework (ZIF-8) for electrochemical and optical detection of AβO [71]. As illustrated in Figure 3, numerous Fc molecules were in-situ encapsulated into the porous ZIF-8. The strong interaction between Zn ions and AβO could break the structure of ZIF-8 and led to the release of Fc molecules into solution. Fc with electrochemical and optical activity could generate corresponding signals for AβO detection. AuNPs can act as nanocarriers for electroactive Fc molecules to amplify the current signal. For instance, Deng et al. constructed an electrochemical aptasensor for AβO detection by using aptamer-labeled Fc@streptavidin(SA)-AuNPs [76]. Yu et al. proposed an electrochemical method for the detection of $Aβ_{(1-40/1-42)}$ by using Th and gelsolin-labeled AuNPs [72]. As illustrated in Figure 4, SPCEs was modified with multiwalled carbon nanotubes (MWCNTs) and AuNPs. Gelsolin was further immobilized on the surface for the capture of $Aβ_{(1-40/1-42)}$ based on the specificity of gelsolin for Aβ. Moreover, AuNPs modified with Th and gelsolin were used to label and detect $Aβ_{(1-40/1-42)}$. This method could sensitively and simply detect $Aβ_{(1-40/1-42)}$ without the use of antibodies and aptamers. To accurately assess the dynamic formation of oligomeric and fibrillar Aβ aggregates, Yu et al. developed a two-channel electrochemical immunosensor for the determination of AβO and AβF [77]. As presented in Figure 5, nanostructured lipid carrier (NLC) was utilized to load Th and two types of polyclonal antibodies (A11 of anti-oligomer and OC of anti-fibril). The electrode was modified with nanocomposite of polymeric ionic liquid and carbon nanotube (CNT). Based on the traditional dual-antibody sandwich strategy, two targets were analyzed simultaneously and the ratio of AβF to AβO was calculated. They demonstrated that the level of AβO decreased and that of AβF increased with the gradual self-aggregation of Aβ.

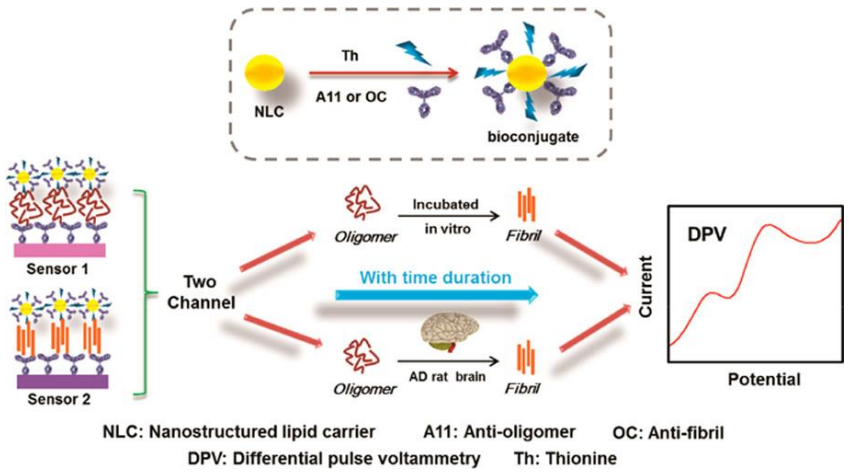

Figure 5. Schematic illustration of the sensing of AβOs and AβFs in the two-channel electrochemical system [77]. Copyright 2019 American Chemical Society.

Phosphorylated Aβ (pAβ) can significantly accelerate the generation and stabilization of AβO with increased toxicity. To accurately evaluate the ratio of pAβ to total Aβ (pAβ/tAβ), Yin et al. reported

an electrochemical assay for coimmunocapture and determination of total $A\beta_{1\text{-}40}$ and $pA\beta_{1\text{-}40}$ [78]. As shown in Figure 6, TiP nanospheres were synthesized and decorated with Cd^{2+}/Ti^{4+} ions (Cd^{2+}/Ti^{4+}@TiP). After the synchronously immunocapture by anti-$A\beta_{1\text{-}40}$ antibody-modified gold electrode, the level of total $A\beta_{1\text{-}40}$ was analyzed by the electrochemical impedance spectroscopy (EIS). Then, Cd^{2+}/Ti^{4+}@TiP was introduced to specifically label the captured $pA\beta_{1\text{-}40}$ via the interaction between Ti^{4+} ions and phosphorous groups on $pA\beta_{1\text{-}40}$ surface. Numerous Cd^{2+} ions in TiP nanospheres could produce strong electrochemical signal to indicate the concentration of $pA\beta_{1\text{-}40}$ monomers in total captured $A\beta_{1\text{-}40}$. Recently, Huang et al. designed a signal amplification strategy for AβO detection based on the self-assembly of peptide [79]. In this study, after being captured by a cysteine-containing peptide CP4-PrP(95–110), AβO could be recognized by Fc-conjugated peptide C16-GGGPrP(95–110)-Fc that further induced the in-situ assembly of more C16-GGGPrP(95–110)-Fc. The formed nanofibers contained a large number of Fc molecules, thus amplifying the electrochemical signal.

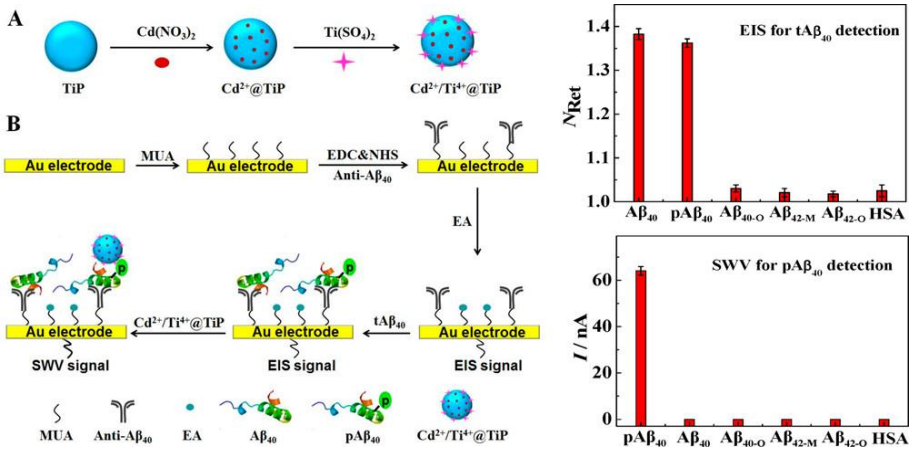

Figure 6. Schematic illustration of the electrochemical detection of $tA\beta_{40}$ and $pA\beta_{40}$. (**A**) Preparation of Cd^{2+}/Ti^{4+}@TiP. (**B**) Construction and detection principle of the electrochemical sensor [78]. Copyright 2019 American Chemical Society.

2.3 Other nanomaterials-based methods

As one family of "artificial or plastic antibodies", molecularly imprinted polymers (MIPs) can be utilized to specific recognize and capture targets. Because of their advantages of high selectivity, excellent stability and broad applicability, MIPs have been integrated into electrochemical sensors/biosensors [80]. For example, You et al. fabricated a MIPs and aptamer-based sandwich electrochemical biosensor for AβO detection [81]. In this study, MIPs film was fabricated on the AuNPs-GO-modified electrode to capture AβO. Then, aptamer-conjugated SiO_2@AgNPs were added to label AβO and generated electrochemical signal. Moreover, Moreira et al. developed an electrochemical sensor of $A\beta_{1\text{-}42}$ based on plastic antibodies on Cu@CNTs [82].

In recent years, miniaturized electrochemical sensors integrated with microfluidics have received more and more attentions because of the advantages of high sensitivity, requirement of low volume samples and time saving [83]. Kasturi et al. have fabricated a microvalve-controlled miniaturized electrochemical lab-on-a-chip for the detection of $A\beta_{1\text{-}42}$ [84]. Field effect transistor (FET) combining

with immunoaffinity biosensor have also been used for the detection of targets by recording the change of the electrical conductance. Oh et al. reported a CNT-based metal semiconductor FET for Aβ detection [85]. They demonstrated that the immobilization of antibody through an antibody-binding protein could enhance the detection performance, compared with that of covalent linkage.

Table 2. Analytical performances of various electrochemical biosensors for Aβ detection with nanomaterials as the signal reporters.

Signal label	Target	Detection limit	Linear range	Ref.
AuNPs	AβO	45 pM	0.0001–0.1 μM	[60]
AuNPs	AβO	0.5 fM	0.001–10 pM	[61]
AuNPs	Aβ	19 pg/mL	0.02–12.5 ng/mL	[63]
Aβ(1–16)-heme-modified AuNPs	Aβ	10 pM	0.02–1.5 nM	[64]
CuCo-CeO_2-Pd	Aβ	0.05 pM	0.001–100 nM	[62]
Au-Cu_xO@m-CeO_2	Aβ	0.036 pg/mL	1×10^{-4}–10 ng/mL	[65]
AuNPs-accelerated Ag deposition	Aβ	0.2 pM	0.001–50 nM	[67]
polyT-templated CuNPs	AβO	3.5 pM	10–2200 pM	[68]
AuNPs/Cu-MOFs	AβO	0.45 nM	0.001–2 μM	[69]
AuNPs@CuMOF	AβO	0.25 fM	0.5–500 fM	[70]
Ad-PrP(95−110)-AgNPs	AβO	8 pM	0.02–100 nM	[66]
AuNPs-Th	AβO	100 pM	0.5–30 nM	[73]
Cu-Al_2O_3-g-C_3N_4-Pd and UiO-66@PANI-MB	Aβ	0.0033 pg/mL	1×10^{-5}–100 ng/mL	[74]
Fc-MOF	Aβ	0.03 pg/mL	0.0001–100 ng/mL	[75]
Fc-ZIF-8	AβO	10 pM	0.01–100 μM	[71]
Fc@SA-AuNPs	AβO	93.0 pM	0.0001–1 μM	[76]
Th and gelsolin-labeled AuNPs	$Aβ_{(1-40/1-42)}$	50 pM	0.2–40 nM	[72]
AuNPs-Th	AβO and AβF	0.01 ng/mL(AβO); 0.02 pg/mL (AβF)	0.2–40 ng/mL	[77]
Cd^{2+}/Ti^{4+}@TiP	total $Aβ_{1-40}$ and $pAβ_{1-40}$	0.45 fM	50–700 pM ($Aβ_{1-40}$); 0.001–100 pM ($pAβ_{1-40}$)	[78]
peptide nanofibers	AβO	0.6 nM	0.005–5 μM	[79]

Abbreviation: AuNPs, gold nanoparticles; AβO, Aβ oligomer; MOF, metal organic framework; Ad, adamantine; Th, thionine; PANI, polyaniline; MB, methylene blue; Fc, ferrocene; ZIF-8, zeolitic imidazole framework; SA, streptavidin; polyT, poly(thymine); CuNPs, Cu nanoparticles.

3. CONCLUSION

In summary, the development of nanomaterials-based electrochemical biosensors for the detection of Aβ species was overviewed. Nanomaterials with excellent electroactivity and electrocatalytic properties have provided a novel and potential signal amplification strategy with

improving sensitivity. Nevertheless, there is still more room for the improvement in the combination of nanomaterials with biosensors, in especial repeatability and long-term stability.

ACKOWLEDGMENTS
This work was supported by the National Natural Science Foundation of China (U2004193).

References

1. C. Janus, J. Pearson, J. McLaurin, P. M. Mathews, Y. Jiang, S. D. Schmidt, M. A. Chishti, P. Horne, D. Heslin, J. French, H. T. Mount, R. A. Nixon, M. Mercken, C. Bergeron, P. E. Fraser, P. St George-Hyslop and D. Westaway, *Nature*, 408 (2000) 979.
2. J. Hardy and D. J. Selkoe, *Science*, 297 (2002) 353.
3. U. Sengupta, A. N. Nilson and R. Kayed, *EBioMedicine*, 6 (2016) 42.
4. C. Haass and D. J. Selkoe, *Nat Rev Mol Cell Biol*, 8 (2007) 101.
5. Y. Zhang, B. Ren, D. Zhang, Y. Liu, M. Zhang, C. Zhao and J. Zheng, *J. Mater. Chem. B*, 8 (2020) 6179.
6. P. Inbar, M. R. Bautista, S. A. Takayama and J. Yang, *Anal Chem*, 80 (2008) 3502.
7. K. A. Bruggink, W. Jongbloed, E. A. Biemans, R. Veerhuis, J. A. Claassen, H. B. Kuiperij and M. M. Verbeek, *Anal. Biochem.*, 433 (2013) 112.
8. W. K. Fang, L. Liu, L. L. Zhang, D. Liu, Y. Liu and H. W. Tang, *Anal. Chem.*, 93 (2021) 12447.
9. J. Zhou, L. Meng, W. Ye, Q. Wang, S. Geng and C. Sun, *Anal Chim Acta*, 1022 (2018) 124.
10. T. Hu, S. Lu, C. Chen, J. Sun and X. Yang, *Sens. Actuat. B: Chem.*, 243 (2017) 792.
11. C. Deng, H. Liu, M. Zhang, H. Deng, C. Lei, L. Shen, B. Jiao, Q. Tu, Y. Jin, L. Xiang, W. Deng, Y. Xie and J. Xiang, *Anal. Chem.*, 90 (2018) 1710.
12. E. J. Blackie, E. C. Le Ru and P. G. Etchegoin, *J. Am. Chem. Soc.*, 131 (2009) 14466-14472.
13. A. Ali, J. Zhao, M. S. Khan, H. Wang, X. Ren, L. Hu, R. Manzoor, D. Wu and Q. Wei, *Sens. Actuat. B: Chem.*, 329 (2021) 129155.
14. L. Yin, Y. Wang, R. Tan, H. Li and Y. Tu, *Microchim. Acta*, 188 (2021) 53.
15. J. Zhang, X. Zhang, Y. Gao, J. Yan and W. Song, *Biosens. Bioelectron.*, 176 (2021) 112945.
16. N. Zhang, Y. Wang, G. Zhao, C. Wang, Y. Li, Y. Zhang, H. Wang and Q. Wei, *Analyst*, 145 (2020) 619.
17. M. Korecka and L. M. Shaw, *J. Neurochem.*, 159 (2021) 211.
18. M. Schaier, G. Hermann, G. Koellensperger and S. Theiner, *Anal. Bioanal. Chem.*, 414 (2022) 639.
19. X. Cheng and R. B. van Breemen, *Anal. Chem.*, 77 (2005) 7012.
20. L. M. T. Phan, T. X. Hoang, T. A. T. Vo, H. L. Pham, H. T. N. Le, S. R. Chinnadayyala, J. Y. Kim, S. M. Lee, W. W. Cho, Y. H. Kim, S. H. Choi and S. Cho, *Expert Rev. Mol. Diagn.*, 21 (2021) 175.
21. E. Mikula, *Curr. Med. Chem.*, 28 (2021) 4049.
22. S. Li and K. Kerman, *Biosens. Bioelectron.*, 179 (2021) 113035.
23. C. Toyos-Rodriguez, F. J. Garcia-Alonso and A. de la Escosura-Muniz, *Sensors*, 20 (2020) 4748.
24. J. Qin, J. S. Park, D. G. Jo, M. Cho and Y. Lee, *Sens. Actuat. B: Chem.*, 273 (2018) 1593.
25. E. Mikula, M. Sulima, I. Marszalek, A. Wyslouch-Cieszynska, P. Verwilst, W. Dehaen, J. Radecki and H. Radecka, *Sensors*, 13 (2013) 11586.
26. M. Vestergaard, K. Kerman, M. Saito, N. Nagatani, Y. Takamura and E. Tamiya, *J Am Chem Soc*, 127 (2005) 11892.
27. Y. Zhang, G. Figueroa-Miranda, Z. Lyu, C. Zafiu, D. Willbold, A. Offenhäusser and D. Mayer,

Sens. Actuat. B: Chem., 288 (2019) 535.
28. Z. Norazreen and M. Z. Zainiharyati, *Int. J. Electrochem. Sci.*, 11 (2016) 872-881.
29. J. S. Park, H. J. Kim, J. H. Lee, J. H. Park, J. Kim, K. S. Hwang and B. C. Lee, *Sensors*, 18 (2018) 426.
30. Y. Zhang, G. Figueroa-Miranda, C. Wu, D. Willbold, A. Offenhausser and D. Mayer, *Nanoscale*, 12 (2020) 16501.
31. A. J. Veloso, A. M. Chow, H. V. Ganesh, N. Li, D. Dhar, D. C. Wu, S. Mikhaylichenko, I. R. Brown and K. Kerman, *Anal. Chem.*, 86 (2014) 4901.
32. Y. R. Wang, H. C. Chuang, A. Tripathi, Y. L. Wang, M. L. Ko, C. C. Chuang and J. C. Chen, *Anal. Chem.*, 93 (2021) 8099.
33. J. Qin, D. G. Jo, M. Cho and Y. Lee, *Biosens. Bioelectron.*, 113 (2018) 82.
34. H. T. N. Le, J. Park and S. Cho, *Micromachines*, 11 (2020) 791.
35. H. T. Ngoc Le, J. Park, S. R. Chinnadayyala and S. Cho, *Biosens. Bioelectron.*, 144 (2019) 111694.
36. J. V. Rushworth, A. Ahmed, H. H. Griffiths, N. M. Pollock, N. M. Hooper and P. A. Millner, *Biosens. Bioelectron.*, 56 (2014) 83.
37. Y. Duan, J. Chen, Y. Jin, Q. Tu, S. Wang and J. Xiang, *Anal. Chem.*, 93 (2021) 3611.
38. S. Prabhulkar, R. Piatyszek, J. R. Cirrito, Z. Z. Wu and C. Z. Li, *J. Neurochem.*, 122 (2012) 374.
39. H. Li, Y. Cao, X. Wu, Z. Ye and G. Li, *Talanta*, 93 (2012) 358.
40. Y. Zhang, G. Figueroa-Miranda, C. Zafiu, D. Willbold, A. Offenhausser and D. Mayer, *ACS Sens.*, 4 (2019) 3042.
41. X. Liao, C. Zhang, Z. Shi, H. Shi, Y. Qian and F. Gao, *J. Electroanal. Chem.*, 878 (2020) 114604.
42. L. Liu, Q. He, F. Zhao, N. Xia, H. Liu, S. Li, R. Liu and H. Zhang, *Biosens. Bioelectron.*, 51 (2014) 208.
43. L. Liu, N. Xia, M. Jiang, N. Huang, S. Guo, S. Li and S. Zhang, *J. Electroanal. Chem.*, 754 (2015) 40.
44. Y. M. Park, J. Ahn, Y. S. Choi, J. M. Jeong, S. J. Lee, J. J. Lee, B. G. Choi and K. G. Lee, *Nano Converg.*, 7 (2020) 29.
45. T. C. Liu, Y. C. Lee, C. Y. Ko, R. S. Liu, C. C. Ke, Y. C. Lo, P. S. Hong, C. Y. Chu, C. W. Chang, P. W. Wu, Y. Y. Chen and S. Y. Chen, *Theranostics*, 8 (2018) 4210.
46. M. Negahdary and H. Heli, *Microchim. Acta*, 186 (2019) 766.
47. M. Negahdary and H. Heli, *Talanta*, 198 (2019) 510.
48. G. Palla, K. Malecka, W. Dehaen, J. Radecki and H. Radecka, *Bioelectrochemistry*, 137 (2021) 107643.
49. J. Qin, S. Kim, M. Cho and Y. Lee, *Chem. Eng. J.*, 401 (2020) 126055.
50. Y. Yu, X. Sun, D. Tang, C. Li, L. Zhang, D. Nie, X. Yin and G. Shi, *Biosens. Bioelectron.*, 68 (2015) 115.
51. M. Chikae, T. Fukuda, K. Kerman, K. Idegami, Y. Miura and E. Tamiya, *Bioelectrochemistry*, 74 (2008) 118.
52. E. C. Rama, M. B. González-García and A. Costa-García, *Sens. Actuat. B: Chem.*, 201 (2014) 567.
53. P. Supraja, S. Tripathy, S. R. K. Vanjari, R. Singh, V. Singh and S. G. Singh, *Sens. Actuat. B: Chem.*, 346 (2021) 130522.
54. F. S. Diba, S. Kim and H. J. Lee, *Catalysis Today*, 295 (2017) 41.
55. Y. Liu, Q. Xu, Y. Zhang, B. Ren, L. Huang, H. Cai, T. Xu, Q. Liu and X. Zhang, *Talanta*, 231 (2021) 122360.
56. H. Y. Abbasi, Z. Tehrani, A. Devadoss, M. M. Ali, S. Moradi-Bachiller, D. Albani and O. J. Guy, *Nanoscale Adv.*, 3 (2021) 2295.

57. J. Sethi, M. Van Bulck, A. Suhail, M. Safarzadeh, A. Perez-Castillo and G. Pan, *Microchim. Acta*, 187 (2020) 288.
58. R. Devi, S. Gogoi, H. S. Dutta, M. Bordoloi, S. K. Sanghi and R. Khan, *Nanoscale Adv.*, 2 (2020) 239.
59. S. S. Li, C. W. Lin, K. C. Wei, C. Y. Huang, P. H. Hsu, H. L. Liu, Y. J. Lu, S. C. Lin, H. W. Yang and C. C. Ma, *Sci. Rep.*, 6 (2016) 25155.
60. N. Xia, X. Wang, J. Yu, Y. Wu, S. Cheng, Y. Xing and L. Liu, *Sens. Actuat. B: Chem.*, 239 (2017) 834.
61. X. Wang, X. Gu, L. Li, B. Yu, L. Lv, Q. Chen and M. Xu, *Anal. Bioanal. Chem.*, 413 (2021) 3707.
62. K. Cui, C. Zhou, B. Zhang, L. Zhang, Y. Liu, S. Hao, X. Tang, Y. Huang and J. Yu, *ACS Appl. Mater. Inter.*, 13 (2021) 33937.
63. A. de la Escosura-Muniz, Z. Plichta, D. Horak and A. Merkoci, *Biosens. Bioelectron.*, 67 (2015) 162.
64. L. Liu, F. Zhao, F. Ma, L. Zhang, S. Yang and N. Xia, *Biosens. Bioelectron.*, 49 (2013) 231.
65. Z. Gao, Y. Li, C. Zhang, S. Zhang, Y. Jia, F. Li, H. Ding, X. Li, Z. Chen and Q. Wei, *ACS Appl. Mater. Inter.*, 11 (2019) 12335.
66. N. Xia, X. Wang, B. Zhou, Y. Wu, W. Mao and L. Liu, *ACS Appl. Mater. Inter.*, 8 (2016) 19303.
67. S. Ding, Y. Xu, Q. Liu, H. Gu, A. Zhu and G. Shi, *Analyst*, 145 (2020) 2331.
68. Y. Zhou, Y. Lv, H. Dong, L. Liu, G. Mao, Y. Zhang and M. Xu, *Sens. Actuat. B: Chem.*, 331 (2021) 129429.
69. Y. Zhou, C. Li, X. Li, X. Zhu, B. Ye and M. Xu, *Anal. Methods*, 10 (2018) 4430.
70. X. Wang, L. Li, X. Gu, B. Yu and M. Jiang, *Microchim. Acta*, 188 (2021) 49.
71. J. Qin, M. Cho and Y. Lee, *ACS Appl. Mater. Inter.*, 11 (2019) 11743.
72. Y. Yu, L. Zhang, C. Li, X. Sun, D. Tang and G. Shi, *Angew. Chem. Int. Ed.*, 53 (2014) 12832.
73. Y. Zhou, H. Zhang, L. Liu, C. Li, Z. Chang, X. Zhu, B. Ye and M. Xu, *Sci. Rep.*, 6 (2016) 35186.
74. J. Miao, X. Li, Y. Li, X. Dong, G. Zhao, J. Fang, Q. Wei and W. Cao, *Anal. Chim. Acta*, 1089 (2019) 48.
75. J. Han, M. Zhang, G. Chen, Y. Zhang, Q. Wei, Y. Zhuo, G. Xie, R. Yuan and S. Chen, *J. Mater. Chem. B*, 5 (2017) 8330.
76. C. Deng, H. Liu, S. Si, X. Zhu, Q. Tu, Y. Jin and J. Xiang, *Microchim. Acta*, 187 (2020) 239.
77. Y. Yu, T. Yin, Q. Peng, L. Kong, C. Li, D. Tang and X. Yin, *ACS Sens.*, 4 (2019) 471.
78. Z. Yin, S. Wang, B. Shen, C. Deng, Q. Tu, Y. Jin, L. Shen, B. Jiao and J. Xiang, *Anal. Chem.*, 91 (2019) 3539.
79. Y. Huang, B. Zhang, L. Yuan and L. Liu, *Sens. Actuat. B: Chem.*, 335 (2021) 129697.
80. F. T. C. Moreira and M. G. F. Sales, *Sens. Actuat. B: Chem.*, 240 (2017) 229.
81. M. You, S. Yang, Y. An, F. Zhang and P. He, *J. Electroanal. Chem.*, 862 (2020) 114017.
82. F. T. C. Moreira, B. A. G. Rodriguez, R. A. F. Dutra and M. G. F. Sales, *Sens. Actuat. B: Chem.*, 264 (2018) 1.
83. K. Islam, Y. C. Jang, R. Chand, S. K. Jha, H. H. Lee and Y. S. Kim, *J. Nanosci. Nanotechnol.*, 11 (2011) 5657.
84. S. Kasturi, S. R. Torati, Y. Eom and C. Kim, *J. Ind. Engin. Chem.*, 97 (2021) 349.
85. J. Oh, G. Yoo, Y. W. Chang, H. J. Kim, J. Jose, E. Kim, J. C. Pyun and K. H. Yoo, *Biosens. Bioelectron.*, 50 (2013) 345.